Scaling Laws for Testing Airfoils Under Heavy Rainfall

Alan J. Bilanin*
Continuum Dynamics, Inc., Princeton, New Jersey

Subscale test data have shown that airfoils operating in a simulated heavy-rain environment can experience significant performance penalties. The physical mechanism resulting in this performance penalty has yet to be conclusively identified. Therefore, the extrapolation of subscale data to full-scale conditions must be undertaken with extreme caution since complete scaling laws are unknown. This paper discusses some of the technical issues that must be addressed and resolved prior to extrapolating the performance of full-scale airfoils from subscale test data. A set of scaling laws is suggested based on the neglect of thermodynamic interactions between the droplets and the air/water vapor phase.

Nomenclature

a = isentropic acoustic speed
c = airfoil chord
C_d = drag coefficient
C_L = lift coefficient
c_v = specific heat at constant volume
D = drop diameter
h_{fg} = latent heat of vaporization of water
ℓ = mean distance between droplets
m = mass
M = Mach number
$n(D)$ = raindrop size spectrum
n_0 = 8×10^3 m^{-3}mm^{-1} = n_{0fs}
N = aerodynamic force
ND = droplet number density
p = pressure
R = rainfall rate, mm/h, or gas constant
T = temperature
u_i = velocity vector
U_∞ = flight speed
V = volume or droplet impact velocity
V_T = drop terminal velocity
W_L = liquid water content, g/m^3
We = Weber number
x,y,z = Cartesian coordinate system
α = angle of attack
β = impact angle
γ = ratio of specific heat
θ = contact angle
Λ = reciprocal of rain spectrum scale
μ = absolute viscosity
ν = kinematic viscosity
ρ = density
σ = surface tension
τ = shear stress
Φ = velocity potential

Subscripts

a = air
fs = full scale
ss = subscale
s = solid
v = vapor
w = water

Presented as Paper 85-0257 at the AIAA 23rd Aerospace Sciences Meeting, Reno, NV, Jan. 14–17, 1985; received July 30, 1985; revision submitted Sept. 11, 1986.
*Senior Associate. Member AIAA.

Introduction

THE National Aeronautics and Space Administration (NASA) and other agencies are currently conducting studies on the performance penalties that might occur when airfoils operate under heavy-rain conditions. The studies to date are primarily of an experimental nature and, for practical reasons, are conducted at subscale. Since incorrect extrapolation of test results to full scale can seriously impact performance predictions, it is critical to have in hand detailed scaling laws. These laws will assure that tests conducted at subscale are relevant to the performance of aircraft.

The effect of rainfall about aircraft has received considerable attention in the literature. However, the bulk of this work is concerned with rain erosion resulting from high-speed droplet impacts with the aircraft surface.[1] The first reported investigation of the effect of heavy rain on the performance of aircraft was published in 1941 by Rhode.[2] In this report, the author concludes that the added drag of rain impacting the aircraft exacted the greatest performance penalty, but that this penalty did not seem to be a safety concern. This conclusion, however, was reached without considering the decreased performance margins that exist during landing. This author has been unable to find any additional published work until 1983 when Luers and his colleague Haines published two articles discussing heavy rain penalties on aircraft,[3,4] followed by a subsequent article by Luers.[5] The conclusion of this work was that, under extremely heavy rain, the rain-roughened wing could suffer a decrease in stall angle with maximum lift coefficient reductions of 30%. In the same time period, Calarese and Hankey[6] published an analytic study showing that, under heavy-rain conditions, the lift of an airfoil actually increased. However, their analysis neglected the droplet interactions with the wing surface and the resulting splash-back and surface roughing effects.

The remaining published investigations on performance penalties associated with operation under heavy-rain conditions were presented at an AIAA meeting in 1985. They include the results of a recent test program conducted by NASA[7,8] on a flapped NACA 64-210 section. These tests confirm at subscale that performance penalties can occur when the airfoil is operating in very severe rainfall. Another paper demonstrates that under heavy-rain conditions, laminar airfoils such as those used on gliders, but tested at subscale, are also susceptible to a performance penalty.[9]

It is clear from the above that performance penalties on airfoils have been identified in subscale tests. Therefore, it is of great importance that scaling laws be developed to aid in the extrapolation of these data to full-scale. This paper attempts to develop scaling laws for testing subscale airfoils under heavy-rain conditions.

Rain Statistics

Anyone who has been caught in a downpour will attest to the fact that the experience is equivalent to standing under a waterfall. In reality, the volume occupied by water is quite small. Under the most severe rainfalls ever recorded, rates have never exceeded 1872 mm/h with a liquid-water content of only 80 g/m^3. Since the density of water is 1 g/cm^3, the volume fraction occupied by water is of the $\mathcal{O}(10^{-4})$ and the water/air mixture is quite dilute. To further emphasize the dilute nature of the mixture, raindrop diameter spectrums have been measured to be in the range 0.1–6.0 mm, with the larger diameters associated with the heaviest rainfalls. Assuming a 4 mm average diameter drop, the mean distance between drops corresponding to a liquid-water content of 80 g/m^3 and a rainfall rate of 1872 mm/h is of the order of 7 cm. Rain rates of 1 cm/h are considered a heavy shower. The average distance between drops as a function of drop diameter and rainfall rate is summarized in Fig. 1. Note again that observation has shown that the heaviest rainfall rates are correlated with the largest drop diameters. Since wing thickness is of the order of a fraction of a meter, several drops will impact the wing more or less simultaneously. It is clear that if subscale testing is undertaken without changing the mean distance between drops, it is possible to pick a scale below which impacts become infrequent. As will be shown, this observation will have strong implications with regard to choosing a scaling methodology and hints that exact similitude may not be achieved during subscale tests.

The widely used raindrop size spectra is that given by Marshall et al.,[10]

$$n(D) = n_0 \exp(-\Lambda D) \tag{1}$$

where $n(D)$ is the size distribution in terms of the number of drops per cubic meter of air per unit size interval, $\Lambda = 4.1R^{-0.21}$ mm^{-1} and $n_0 = 8\times10^3$ m^{-3}mm^{-1}. R is the rainfall rate in millimeters/hour. The liquid-water content that will become a critical scaling parameter is obtained by integration,

$$W_L(\text{g/m}^3) = \frac{\pi}{6}\times 10^3 \rho_w \int_0^\infty D^3 n(D)\,\mathrm{d}D \tag{2}$$

where the density of water is in grams/cubic centimeter.

The terminal velocity of a raindrop is a function of droplet size and altitude and has been established by Markowitz.[11] At low altitudes, which are of interest here,

$$V_T(\text{m/s}) = 9.58\left\{1 - \exp\left[-\left(\frac{D(\text{mm})}{1.77}\right)^{1.147}\right]\right\} \tag{3}$$

For large drop diameters, say $D = 6$ mm, the terminal velocity is 9.4 m/s. Since aircraft approach landing speeds are of the order of 60 m/s, under the heaviest rainfalls, raindrops impact an airplane at an angle from the horizontal at less than 10 deg. Droplets greater than approximately 10 cm are hydrodynamically unstable and break up.[12]

Airfoil Operation in Heavy Rain

Three companion papers[7-9] describe subscale test programs where aerodynamic performance was measured under simulated heavy-rain conditions. These test programs were conducted in wind tunnels and the rainfall was simulated using water sprays upstream of the model. A qualitative description of some of the observations is given here to introduce the complex physical processes observed when rain is introduced into the flowfield. Referring to Fig. 2, as rain droplets impact the leading-edge region of the airfoil, a fog layer (coined the "ejecta fog") forms. This fog layer is made visible by light scattered from very fine droplets that are produced and splashed back as a consequence of the high-speed impact of the rain droplet. An estimate of the minimum ejecta droplet size that can be produced as a result of the impact is obtained by equating the kinetic energy of the incoming droplet to the surface energy of the ejecta. This estimate assumes that no energy is lost in the impact and that the ejecta have no kinetic energy, so that all available energy is used to break up the droplet. Equating energy and conserving mass yields for the estimate of the minimum droplet diameter results in

$$D_{\min} = 12\sigma_{w,a}/\rho_w U_\infty^2 \tag{4}$$

The maximum size of the ejecta droplets can be estimated by a statement of the incipient instability expected when the drag stresses on the droplet exceed the surface tension stress. Assume that the ejecta droplet is at a point on its trajectory where it is stationary relative to the airfoil. Neglecting the airfoil-induced velocities at this point, the drag force on the ejecta droplet equated to the surface tension force holding the droplet together is

$$\sigma_{w,a}\pi D_{\max} = C_D \frac{1}{2}\rho_a U_\infty^2 \frac{\pi D^2{}_{\max}}{4} \tag{5}$$

Solving for the maximum ejecta diameter yields

$$D_{\max} = 8\sigma_{w,a}/C_D\rho_a U_\infty^2 \tag{6}$$

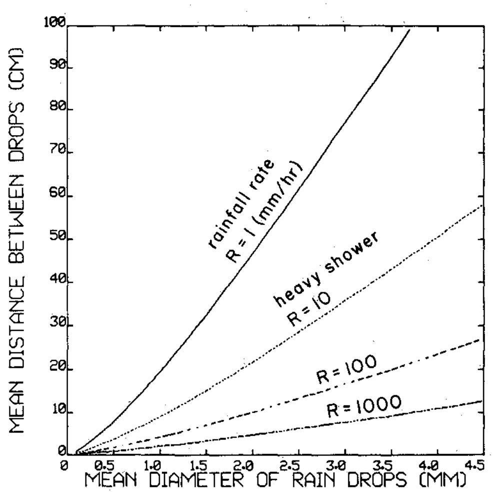

Fig. 1 Mean distance between raindrops as a function of rainfall rate and drop diameter.

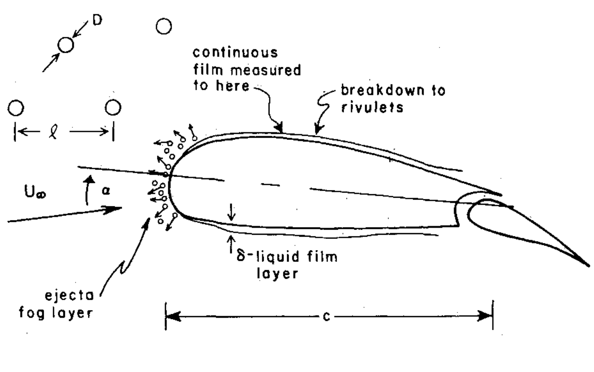

Fig. 2 Idealization of raindrops interacting with an airfoil.

Assuming $C_D = \mathcal{O}(1.0)$ and a landing speed of $U_\infty = 60$ m/s, $D_{min} \simeq 1$ μm and $D_{max} \simeq 100$ μm so that a 4 mm diameter raindrop would break into at least 50×10^3 ejecta droplets. This assumes, of course, that the impact would eject all of the impacting mass. In reality, the maximum diameter of ejecta droplets will be smaller perhaps by as much as a factor of three or four, since around the leading edge of an airfoil the fluid velocities exceed the freestream (neglecting the stagnation region).

The surface area increase of the ejecta over that of the impacting droplet is quite significant and it is estimated for a 4 mm impacting droplet to be 2×10^3. This enormous area increase has implications with regard to evaporation processes in the airfoil's turbulent boundary layer. Estimates using a droplet evaporation model proposed by Fuchs[13] suggest that a sufficiently long time exists, as the ejecta traverse the airfoil's chord, to saturate the boundary layer, even assuming that the incoming flow is not saturated. A first look at the issue of the thermodynamics of evaporation and condensation on airfoil performance is made in the next section.

The ejecta fog motivates the discussion of a mechanism that may result in early de-energization of the airfoil's boundary layer and, hence, early flow separation. This mechanism is tied to the capture efficiency of the airfoil and, hence, its ability to concentrate droplets and ejecta. When a droplet impacts and splashes back from the airfoil, the airfoil experiences a momentary drag increase as a consequence of the change in momentum of the raindrop. Subsequently, in the area surrounding the impact point, the fluid experiences a body force to accelerate and carry the ejecta along the chord. This body force is of the order of the drag force felt by the airfoil upon impact. While the drag associated with direct droplet impact with the airfoil has been estimated to be insignificant for all but the heaviest rainfalls, the forces on the air during splash back and reacceleration of the ejecta over the airfoil may be sufficient to contribute to early boundary-layer separation. The point here is that it is always the air nearest the airfoil that is called upon to reaccelerate the ejecta. The situation is visualized in Fig. 3 where the impact of large rain droplets (so that they are not turned by the airfoil's flowfield) is schematically illustrated.

A continuous water film layer develops beneath the ejecta fog. On the upper surface, at approximately the point of maximum airfoil thickness, which also roughly corresponds to the point beyond which rain droplet impacts are shadowed by the forward portion of the airfoil, the sheet breaks down into rivulets. Continuous sheet thicknesses were measured to be typically several mils and tend to be thicker on the lower surface of the airfoil. Estimates of film thickness buildup and mechanisms limiting the maximum film thickness are discussed in the next section.

Rivulet flowfields, such as those observed in the NASA test series, are common occurrences on heat exchanger tubes and have received considerable study in the literature since the heat transfer through a surface covered by a film is sufficiently different than that of a dry surface. The formation of rivulets was common to the NASA tests[8] and those conducted by Hansman and Barsotti,[9] except in the test series in which the airfoil was waxed. In this case, beading was observed along the entire upper surface of the airfoil. These beads were associated with the nonwetability of the airfoil surface and suggest that surface tension differences between sub- and full-scale models may be a scaling issue.

The film layer, cratering by droplet impact, and instability and breakup into rivulets all interact with the turbulent boundary-layer dynamics. To first order, it has been postulated[3] that these effects are equivalent to airfoil surface roughness, but the issue of de-energization of the boundary layer as a consequence of splash back and condensation and/or evaporation still complicate the physical mechanism, resulting in the observed boundary-layer separation and resulting lift reduction under heavy-rain conditions.

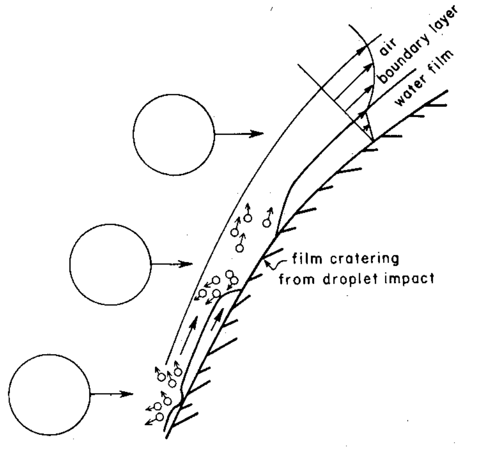

Fig. 3 Idealization of raindrops impacting an airfoil and forming an "ejecta fog" cloud.

Scaling Laws

The flowfield about an airfoil flying through rain is extremely complicated when examined in detail. The thermodynamics of evaporation and/or condensation are coupled to the turbulent flow about the wing; also, droplet impact and splash back must influence the boundary layer. In addition, water film formation on the surface and subsequent breakup into rivulets must also interact to affect the boundary-layer dynamics. In order to make some progress in understanding the test data becoming available, it is prudent to utilize simple limiting analytic models to identify the physical phenomena that are not significant with regard to an airfoil flying in heavy rain. These phenomena may then be neglected during a general scaling analysis.

Thermodynamics of Evaporation and/or Condensation

Under heavy-rain conditions, the air itself may be relatively dry or be completely saturated. In the former case, raindrops impacting the airfoil and splashing back to form an ejecta fog can have sufficient surface area and residence time in the boundary layer to saturate the air. In the latter case, condensation of the saturated boundary-layer flow, as briefly discussed by Luers,[5] might occur. Since it is known that the vapor pressure of water at 20°C is approximately 0.5 psia, the thermodynamics of evaporation and/or condensation in the boundary layer may significantly influence the pressure distribution. This effect can be estimated by treating the thermodynamics of evaporation and/or condensation as a homogeneous equilibrium process and comparing predictions of the pressure distribution about an airfoil with predictions about the same airfoil neglecting evaporation and/or condensation.

Consider the distribution of water droplets in air in a container of volume V and temperature T. If the air is dry and remains so when the volume is changed, the pressure change, assuming isentropic compression of the gas with no phase change, is known to be

$$\mathrm{d}p = -\gamma\rho_a R_a T\frac{\mathrm{d}V}{V} = \gamma R_a T \mathrm{d}\rho_a = a^2 \mathrm{d}\rho_a \tag{7}$$

where γ, R_a, ρ_a are the ratio of specific heats, gas constant, and density of dry air, respectively. The quantity a^2 is the acoustic speed squared and quantifies the magnitude of compressibility of the gas.

An expression similar to Eq. (7) can be derived by assuming that equilibrium evaporation and/or condensation can occur as the pressure is changed. Assuming an isentropic process, which always leaves the air/water vapor saturated, and utilizing the Clausius Clapeyron relation, it may be shown that (see Ref. 14 for details)

$$\mathrm{d}p = a_{\mathrm{eff}}^2 \mathrm{d}\rho \tag{8}$$

where

$$a^2{}_{\mathrm{eff}} = a^2(\rho\alpha/\rho)((1/j) + \{[(j-1)/j][1+(p_v h_{fg}/\rho_a T R_v)] \times [1+(\rho_v/\rho_a)(R_v/R_a)][1-(1-u_{fg}/C_{vw}T) \times \rho_v c_{vw} T/\rho]\}/[1+(\rho_w/\rho_a)(c_{vw}/c_{va}) + (\rho_v c_{vw}/\rho_a c_{va}) \times (1-u_{fg}/c_{vw}T)(1-h_{fg}/R_v T)]) \tag{9}$$

The consequence of the phase change on the lift coefficient is now explored via linear subsonic airfoil theory.

Let the velocity field be defined as the gradient of a potential

$$u_i = \frac{\partial \Phi}{\partial x_i} \tag{10}$$

Then, it is well known that the potential field satisfies

$$(1-M^2)\frac{\partial^2 \Phi}{\partial x^2} + \frac{\partial^2 \Phi}{\partial y^2} + \frac{\partial^2 \Phi}{\partial z^2} = 0 \tag{11}$$

where $M = U_\infty / a$ is the Mach number.

The effect of evaporation and/or condensation is then simply incorporated into linear subsonic airfoil theory by redefining Mach number to be $M_{\mathrm{eff}} = U_\infty / a_{\mathrm{eff}}$.

It is well known that the lift curve slope of a wing operating at M_{eff} is related to the lift curve slope at $M=0$ by

$$\left.\frac{\partial C_L}{\partial \alpha}\right|_{M_{\mathrm{eff}}} = \frac{1}{\sqrt{1-M_{\mathrm{eff}}^2}} \left.\frac{\partial C_L}{\partial \alpha}\right|_{M=0} \tag{12}$$

or if M is the landing Mach number

$$\left.\frac{\partial C_L}{\partial \alpha}\right|_{M_{\mathrm{eff}}} \Big/ \left.\frac{\partial C_L}{\partial \alpha}\right|_{M} = \frac{\sqrt{1-M^2}}{\sqrt{1-M_{\mathrm{eff}}^2}} \tag{13}$$

Substituting nominal thermodynamic values typical of heavy-rain conditions shows that the effective acoustic speed is reduced by approximately 25% or that the effective Mach number is increased by 25%. Therefore, the lift curve slope, under the assumptions made here, is anticipated to increase about 3% during heavy-rain conditions. This prediction is in contradiction to the laminar airfoil data presented by Hansman and Barsotti[9] and strongly suggests that other mechanisms resulting in this observed lift performance penalty must be identified. Since boundary-layer dynamics have been completely neglected in the above analysis, it becomes the prime suspected mechanism. The remainder of this paper addresses scaling of these issues, but omits the issue of evaporation and/or condensation in the boundary layer for the present.

Rainfall and Airfoil Scaling

The object now is to determine the appropriate scaling parameters controlling subscale tests assuming thermodynamic considerations may be neglected. Figure 2 shows a schematic of raindrops of mean diameter D and mean spacing ℓ impacting an airfoil of chord c traveling at velocity U_∞. The airfoil is assumed to be extremely smooth so that physical surface roughness is not a parameter. It is assumed that the tests are to be conducted with a subscale airfoil in air and that rain can be simulated by spraying water from suitably designed and spaced spray nozzles.

The dimensional variables that control the aerodynamic force N generated on the airfoil are shown in Table 1. Note that we have omitted compressibility effects by observing that the landing speeds are slow compared to the speed of sound and omitted gravity by noting that the Froude numbers are very large.

Straightforward application of the Buckingham II theorem yields the fact that the normalized force on the airfoil is a function of nine nondimensional groups,

$$\frac{N}{\rho_a U^2 c^2} = f(\pi_1,\ldots,\pi_9) \tag{14}$$

where

$$\pi_1 = \frac{cU}{\nu_a},\quad \pi_2 = \frac{cU}{\nu_w},\quad \pi_3 = \frac{\rho_w U^2 D}{\sigma_{w,a}}$$
$$\pi_4 = \frac{\sigma_{w,s}}{\sigma_{w,a}},\quad \pi_5 = \frac{\sigma_{a,s}}{\sigma_{w,a}},\quad \pi_6 = \frac{\ell}{c}$$
$$\pi_7 = \frac{D}{c},\quad \pi_8 = \alpha,\quad \pi_9 = \frac{\rho_a}{\rho_w} \tag{15}$$

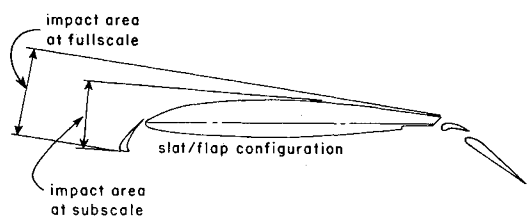

Fig. 4 Geometrically determined impact areas for a 64-210 airfoil at zero angle of attack ($R = 100$ mm/h).

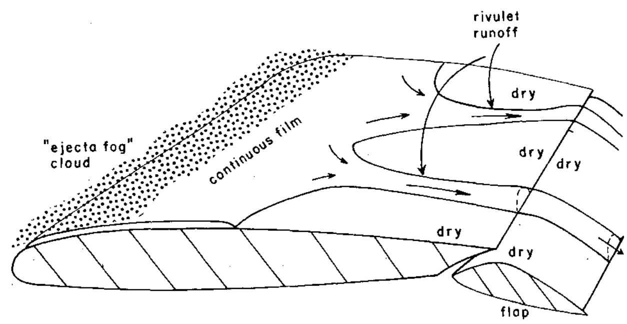

Fig. 5 Observed film flow pattern above a flapped wing.

Table 1 Dimensional variables controlling force N

ρ_a	= density of air, ML^{-3}
ρ_w	= density of water, ML^{-3}
ν_a	= kinematic viscosity of air, L^2T^{-1}
ν_w	= kinematic viscosity of water, L^2T^{-1}
$\sigma_{w,a}$	= surface tension of water/air, MT^{-2}
$\sigma_{w,s}$	= surface tension of water/solid, MT^{-2}
$\sigma_{a,s}$	= surface tension of air/solid, MT^{-2}
D	= volume average drop diameter, L
ℓ	= mean spacing between drops, L
c	= airfoil chord, L
U_∞	= flight speed, LT^{-1}
α	= angle of attack, —
N	= aerodynamic force on airfoil, MLT^{-2}

The first two groups are readily recognized as the Reynolds numbers of the air and water, respectively. Normally, subscale tests distort the Reynolds number, since models are a small fraction of their full-scale size and sufficient tunnel speeds are not available to offset the model size reductions. Without rain, a Reynolds number mismatch is often of little consequence, since the experimentalist resorts to boundary-layer trip devices and demonstrates the insensitivity of measured results to several tunnel speeds. However, with rain present, a second Reynolds number involving the viscosity of water is introduced that is also distorted at subscale. To complicate matters even further, the third scaling parameter is a Weber number squared, which is the ratio of inertial forces to surface tension forces and may not be preserved since the velocity must vary as the square root of the reduction of the physical scale of the experiment. Parameters π_3–π_5 in Eqs. (15) assure that the surface tension forces are properly proportioned to the inertial forces and that these forces will require subsequent discussion since they involve surface wetability and, hence, rivulet formation. Rain geometric parameters π_6 and π_7 dictate that if the airfoil is scaled down, the mean droplet spacing and mean diameter D must also be scaled down.

An immediate consequence of this geometric scaling requirement is that the liquid water content W_L must be preserved between sub- and full scale. Since the terminal velocity of raindrops decreases with decreasing droplet diameters, the rainfall rate R will be reduced during subscale tests. The raindrop spectrum required at subscale is deduced by requiring that the liquid water content be constant between tests and that the droplet number density ND given by

$$\mathrm{ND} = \int_0^\infty n(D)\mathrm{d}D \qquad (16)$$

increase at subscale by the cube of the inverse of the scale factor. Stated mathematically, these two requirements require

$$\int_0^\infty D^3 n_{ss}(D)\mathrm{d}D = \int_0^\infty D^3 n_{fs}(D)\mathrm{d}D$$

$$\int_0^\infty n_{ss}(D)\mathrm{d}D = \left(\frac{c_{fs}}{c_{ss}}\right)^3 \int_0^\infty n_{fs}(D)\mathrm{d}D \qquad (17)$$

where subscripts fs and ss denote full and subscale values, respectively. When evaluated, the above integrals require that the subscale droplet spectrum n_{ss} be prescribed by

$$n_{ss}(D) = n_{0ss}\exp(-\Lambda_{ss}D)$$

$$n_{0ss} = \left(\frac{c_{fs}}{c_{ss}}\right)^4 n_{0fs}$$

$$\Lambda_{ss} = 4.1\frac{c_{fs}}{c_{ss}}R^{-0.21}\mathrm{mm}^{-1} \qquad (18)$$

The rainfall rate at subscale will be less than at full scale and this implies that the effective angle of attack will change between sub- and full-scale tests. The rainfall rate is computed from[12]

$$R(\mathrm{mm/h}) = 6\pi\times10^{-4}\int_0^\infty D^3 n(D)V_T(D)\mathrm{d}D \qquad (19)$$

where V_T is the droplet terminal velocity given by Eq. (3). To check the magnitude of this rainfall distortion, assume that a ¼-scale test is to be conducted simulating a rainfall rate of 100 mm/h. A direct quadrature of Eq. (19), using the spectrum scaling prescribed by Eqs. (18), yields a subscale rainfall rate of 38 mm/h.

At first inspection, this distortion of rainfall rate may seem to be of little signficance. The first-order effect would seem to be the change in the angle at which the rain droplets impact the airfoil. The volume averaged mean drop diameter is computed from

$$D = \int_0^\infty D^4 n(D)\mathrm{d}D \Big/ \int_0^\infty D^3 n(D)\mathrm{d}D = \frac{4}{\Lambda} \qquad (20)$$

which, for a rainfall rate of 100 mm/h, is a $D = 4.9$ mm and a volume-averaged mean drop diameter terminal velocity of 9.2 m/s. At ¼-scale, the volume mean diameter is 1.22 mm and has a terminal velocity of 4.6 m/s. The angles from the horizon at which the rain approaches the airfoil at full and subscale are 8.7 and 4.4 deg, respectively, assuming a 60 m/s landing speed. Figure 4 schematically illustrates the geometrically determined impact areas for the slat/flap airfoil tested at zero angle of attack by Dunham et al.[7] It is not known at this time if any dynamic significance is to be associated with these differences, but rainfall scaling distortions can be investigated quantitatively at subscale by tipping the spray nozzles downward while holding the angle of attack constant.

The remaining two π parameters, angle of attack and density ratio, are matched at subscale and are not discussed further.

Comments on Splash Back, Film Thickness, Rivulets, and Flap Slot Blockage

Having previously noted that the ratio of inertial to viscous forces (Reynolds number) and inertial to surface tension forces (Weber number squared) are likely to be distorted at subscale, it is reasonable to conjecture on the differences anticipated at subscale. Figure 5 is an idealization of the upper surface of an airfoil showing the ejecta region over the forward portion of the wing and a continuous film region to approximately half-chord. The aft section of the airfoil has a rivulet runoff that flows about a flap.

Droplets impacting the airfoil do so at high velocities and the inertial forces at impact totally dominate the surface tension forces. This is seen by computing the Weber number

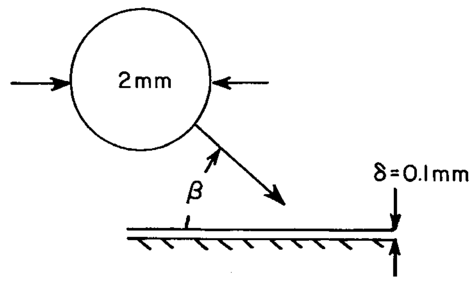

Fig. 6 Scale of rain droplet interacting with wetted airfoil surface.

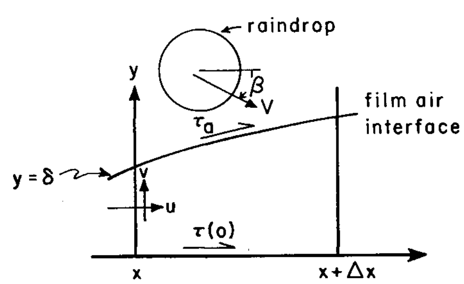

Fig. 7 Control volume for integration of film boundary-layer equations.

squared,

$$We^2 = \rho_w D V^2 / \sigma_{w,a} \tag{21}$$

which for a 2 mm water drop impacting an airfoil at 60 m/s is $\mathcal{O}(10^5)$. Therefore, it is anticipated that the impact dynamics and splash-back pattern should be independent of the impact Weber number for a sufficiently high subscale test impact Weber number and, thus, that the only parameter controlling the ejecta pattern is the incidence angle β. The liquid film on the airfoil surface would seem to complicate this conjecture, but the film thicknesses measured to date for the rainfall rates of interest are much smaller than the droplet diameters.

This is illustrated in Fig. 6 where a scale drawing of a 2 mm diameter raindrop is about to impact a surface with a liquid-film thickness of 4 mils at angle β. Surprisingly little literature has been found dealing with this phenomenon. The work by Rockenbach and Alexander[15] has examined the oblique impact with a moving film and considered the ejecta patterns. Drop sizes were approximately 4 mm and impact velocities were unfortunately low, equal to the terminal velocity of about 9 m/s, while film thicknesses were from one-fourth to four-fourths of the droplet diameter. While the results are not applicable to splash back from an airfoil since the impact velocities are so low, the interesting observation was made that the volume of ejecta droplets exceeded the incoming drop volume. A more relevant work was undertaken in 1975 by Pavarov et al.[16] in the USSR. Here milimeter-sized drops were allowed to impact a rapidly rotating disk and the interaction of the droplet with the boundary layer was investigated by high-speed photography. The incidence angles studied were small so that the droplet had sufficient residence time in the boundary layer to undergo significant distortions. This work should prove useful in understanding the grazing collisions of droplets on the aft upper surface of the wing, but very few details and results are available.

While the initial splash back of the ejecta into the boundary layer is thought to be controlled only by the incidence angle at these high Weber numbers and thin film thicknesses, the interaction of this ejecta with the boundary layer is likely to remain a challenging technical problem for some time to come.

The question of film thickness buildup between subscale and full scale is a critical issue, since high-lift airfoils have slots between the slats and flaps that will be geometrically scaled at subscale. Should subscale film layer thicknesses not scale geometrically, the potential exists to under- or over-block the slots with liquid. Film thickness issues are difficult to address, since film stability from both the stripping of liquid from the film by the airflow and the breakdown to rivulet runoff must also be considered. To see that film thickness issues are a consideration at subscale, a simple analytic model of film thickness buildup is developed here and used to predict results at sub- and full-scale.

Consider the control volume shown in Fig. 7. Rain having a liquid-water content W_L fluxes into the control surface through $y = \delta(x)$. Making the standard boundary-layer approximations in the incompressible two-dimensional Navier-Stokes equations and integrating in the y direction yields for the continuity equation and the x momentum equation,

$$u(\delta)\frac{d\delta}{dx} = v(\delta) + \frac{W_L V}{\rho_w}\sin\beta \tag{22}$$

$$\int_0^\delta 2u\frac{\partial u}{\partial x}dy + u(\delta)^2\frac{d\delta}{dx} - \frac{W_L V^2}{\rho_w}\sin\beta\cos\beta = \frac{\tau(\delta) - \tau(0)}{\rho_w} \tag{23}$$

$\tau(\delta)$ and $\tau(0)$ is the shear stress at $y = \delta$ and 0, respectively. The pressure gradient to be prescribed is taken to be zero. Note that $\tau(\delta)$ is to be specified and results from the airflow above the film. Expressions for the film thickness δ and film velocity u are obtained by assuming that

$$u = U(x)\frac{y}{\delta(x)} \tag{24}$$

The liquid film vertical velocity v is obtained from continuity and Eq. (24)

$$v = \frac{U(x)}{2}\frac{d\delta}{dx} - \frac{\delta}{2}\frac{dU(x)}{dx} \tag{25}$$

Introducing Eqs. (24) and (25) into Eqs. (22) and (23) yields

$$\delta(x)U(x) = \frac{2W_L V}{\rho_w}x\sin\beta \tag{26}$$

$$\frac{d}{dx}(\delta U^2) = \frac{W_L V^2}{\rho_w}\sin\beta\cos\beta + \frac{\tau(\delta)}{\rho_w} - \nu_w\frac{U(x)}{\delta(x)} \tag{27}$$

where $\tau(\delta)$ will be prescribed as the shear stress acting on a turbulent flat plate

$$\tau(\delta) = \frac{0.037\rho_a U_a^2}{(U_a x/\nu_a)^{1/5}}, \quad 5\times10^5 < R_\ell < 10^7 \tag{28}$$

A numerical solution to Eqs. (26–28) is shown on Fig. 8 for the extremely heavy rain conditions tabulated there. The purpose of presenting this film model is not to make absolute predictions of film thickness, but to estimate how significant film thickness scaling will be at subscale.

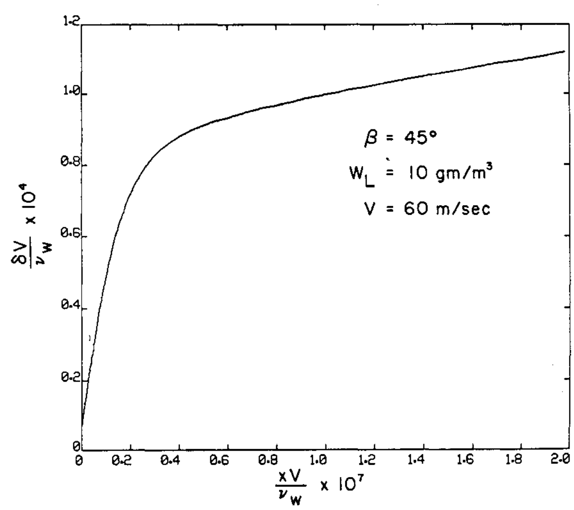

Fig. 8 Nondimensional film thickness as a function of nondimensional downstream distance.

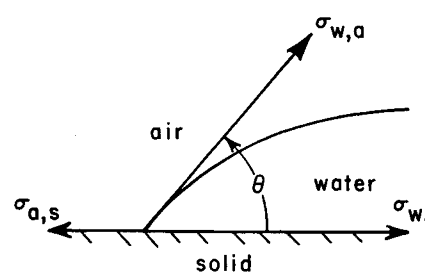

Fig. 9 Definition of contact angle θ.

Assume that a full-scale airfoil has a landing Reynolds number based on wing chord of 10^7 and that a subscale test will be conducted at ¼-scale so that the subscale Reynolds number is 0.25×10^7. From Fig. 8, the nondimensionalized film thicknesses are

$$\left.\frac{\delta}{c}\right|_{ss}\simeq 8000\frac{v_w}{cV_{ss}}$$

$$\left.\frac{\delta}{c}\right|_{fs}\simeq 10000\frac{v_w}{cV_{fs}} \tag{29}$$

Forming the ratio of nondimensional film thickness and substituting full- and subscale Reynolds number yields

$$\frac{(\delta/c)_{ss}}{(\delta/c)_{fs}}\simeq 3 \tag{30}$$

Thus, the subscale airfoil will have a scaled film thickness that is approximately a factor of three too large. The above model, which admittedly does not address ejecta, pressure gradients, and film instability, does indicate that the film thickness and the film blockage of slots between slats and flaps could be a technical issue which must be resolved prior to extrapolation of subscale test data to full scale. The above observation suggests that current subscale test data[6-8] have film thicknesses that are too large. For this reason, it is conjectured that these tests are likely to overestimate the performance penalties associated with operation in heavy rain.

The observed rivulet formation in the tests reported by Hansman and Barsotti[9] and Dunham et al.[7] has been extensively studied in the literature. The most complete analysis of the breakdown of a film driven by external shear was given by Mikielewicz and Moszynski.[17] This analysis equates the kinetic and surface energy of a uniform film to the energy of a rivulet flowfield. In addition, by conserving mass and requiring that the newly formed rivulets assume a minimum energy configuration to be stable, the film thickness δ at which rivulet formation occurs is obtained.

Film thickness at breakdown is related to contact angle θ by

$$\rho_w\tau^2\delta^3/6\mu_w^2\sigma_{w,a}\approx 0.18\theta^2,\ 0<\theta<\pi/2 \tag{31}$$

Referring to Fig. 9, the contact angle is defined by Young's equation and is related to the surface tensions by

$$\sigma_{a,s}-\sigma_{w,s}=\sigma_{w,a}\cos\theta \tag{32}$$

Equation (32) suggests that airfoil wetability should be considered during subscale testing since rivulets introduce significant effective roughness elements to the boundary layer. The above observations are consistent with the findings of Hansman and Barsotti[9] where performance penalties under heavy-rain conditions were shown to be a strong function of airfoil wetability.

Conclusions and Recommendations

Extrapolating airfoil performance data taken at subscale under simulated heavy-rain conditions to full scale must be undertaken with caution. Since both Weber and Reynolds number scaling may not be possible at subscale, boundary-layer and drop and film water layer dynamics could be distorted at subscale. Based on simple analytic models and evaluation of the ¼-scale tests reported by Dunham et al.,[7] it is anticipated that the extrapolation of ¼-scale results to full scale will overestimate the anticipated performance penalties. Additional testing and analysis is strongly warranted to quantify the performance penalty when operating under heavy-rain conditions.

Acknowledgments

The author would like to thank Mr. R. E. Dunham for making data available, his colleagues Drs. D. B. Bliss for technical discussions, and M. E. Teske for numerical results. This work was supported by NASA Purchase Order L71488B.

References

[1]Springer, G. S., *Erosion by Liquid Impact,* Wiley, New York, 1976.

[2]Rhode, R. V., "Some Effects of Rainfall on Flight of Airplanes and on Instrument Indications," NACA TN 803, 1941.

[3]Haines, P. A. and Luers, J. K., "Aerodynamic Penalties of Heavy Rain on a Landing Aircraft," NASA CR 156885.

[4]Luers, J. K. and Haines, P. A., "Experimental Measurements of Rain Effects on Aircraft Aerodynamics," AIAA Paper 83-0275, Jan. 1983.

[5]Luers, J. K., "Heavy Rain Effects on Aircraft," AIAA Paper 83-0206, Jan. 1983.

[6]Calarese, W. and Hankey, W. L., "Numerical Analysis of Rain Effects on an Airfoil," AIAA Paper 84-0539, Jan. 1984.

[7]Dunham, R. E., Bezos, G. M., Gentry, C. L., and Melson, E., "Two-Dimensional Wind Tunnel Tests of a Transport-Type Airfoil in a Water Spray," AIAA Paper 85-0258, Jan. 1985.

[8]Hastings, E. C. and Manuel, G. S., "Scaled Model Tests of Airfoils in Simulated Heavy Rain," *Journal of Aircraft,* Vol. 22, June 1985, pp. 536–540.

[9]Hansman, R. J. and Barsotti, M. F., "Surface Wetting Effects on a Laminar Flow Airfoil in Simulated Heavy Rain," *Journal of Aircraft,* Vol. 22, Dec. 1985, pp. 1049–1053.

[10]Marshall, J. S., Langille, R. C., and Palmer, W. McK., "The Distribution of Raindrops with Size," *Journal of Meteorology,* Vol. 5, 1948, pp. 165–166.

[11]Markowitz, A. M., "Raindrop Size Distribution Expressions," *Journal of Applied Meteorology,* Vol. 15, 1976, pp. 1029–1031.

[12]Pruppacher, H.R., *Microphysics of Clouds and Precipitation,* D. Reidel Publishing, Dordrecht, the Netherlands, 1978.

[13]Fuchs, N. A., *Evaporation and Droplet Growth in Gaseous Media,* Pergamon Press, New York, 1959.

[14]Bilanin, A. J., "Scaling Laws for Testing of High Lift Airfoils Under Heavy Rainfall," AIAA Paper 85-0257, Jan. 1985.

[15]Rockenbach, F. A. and Alexander, D. R., "An Experimental Study of Angular Collisions between Drops and Moving Liquid Films," *Proceedings of ASME-ANS Nuclear Reactor Thermal Hydraulic Topical Meeting,* 1980, pp. 1504–1522.

[16]Pavarov, O. A., Shal'nev, K. K., Nazarov, O. I., and Shalobasov, I. A., "Collision of Droplets with a Moving Plane Surface," *Soviet Physics—Doklady (USA),* Vol. 20, No. 11, 1975, pp. 782–783.

[17]Mikielewicz, J. and Moszynski, J. R., "Breakdown of a Shear Driven Liquid Film," *Prace Instytutu Maszyn Przeplywowych, Polska Akademia Nauk,* Vol. 66, 1975, pp. 3–11.